The DNA helicase ChlR1 is required for sister chromatid cohesion in mammalian cells

Joanna L. Parish[1], Jack Rosa[2], Xiaoyu Wang[1], Jill M. Lahti[3], Stephen J. Doxsey[2] and Elliot J. Androphy[1,*]

[1]Department of Medicine and [2]Program in Molecular Medicine, University of Massachusetts Medical School, Worcester, MA 01605, USA
[3]Department of Genetics and Tumor Cell Biology, St Jude Children's Research Hospital, Memphis, TN 38105, USA
*Author for correspondence (e-mail: elliot.androphy@umassmed.edu)

Accepted 15 September 2006
Journal of Cell Science 119, 4857-4865 Published by The Company of Biologists 2006
doi:10.1242/jcs.03262

Summary

It has recently been suggested that the *Saccharomyces cerevisiae* protein Chl1p plays a role in cohesion establishment. Here, we show that the human ATP-dependent DNA helicase ChlR1 is required for sister chromatid cohesion in mammalian cells. Localization studies show that ChlR1 diffusely coats mitotic chromatin in prophase and then translocates from the chromatids to concentrate at the spindle poles during the transition to metaphase. Depletion of ChlR1 protein by RNA interference results in mitotic failure with replicated chromosomes failing to segregate after a pro-metaphase arrest. We show that depletion also results in abnormal sister chromatid cohesion, determined by increased separation of chromatid pairs at the centromere. Furthermore, biochemical studies show that ChlR1 is in complex with cohesin factors Scc1, Smc1 and Smc3. We conclude that human ChlR1 is required for sister chromatid cohesion and, hence, normal mitotic progression. These functions are important to maintain genetic fidelity.

Key words: Helicase, Cohesion, Cohesin, Mitosis

Introduction

DNA-dependent helicases are a highly conserved class of enzymes that use the energy of ATP hydrolysis to catalyze the unwinding of double- or single-stranded DNA molecules. They are required for nearly every aspect of DNA metabolism including DNA replication, repair, transcription and recombination (Tuteja and Tuteja, 2004) and are essential to all cells. Defects in helicase function in these processes can result in genomic instability and a predisposition to cancer. For example, mutations in the RecQ-like helicases *BLM*, *WRN* and *RECQL4 (RTS)* cause Blooms syndrome, Werner syndrome and Rothmund-Thomson syndrome, respectively, all of which are associated with chromosomal instability and elevated mutation rates (van Brabant et al., 2000).

The DEAH helicase family member ChlR1 binds both single- and double-stranded DNA and possesses both ATPase and DNA helicase activities (Amann et al., 1997; Hirota and Lahti, 2000). ChlR1 expression appears to be ubiquitous with highest levels observed in tissues with rapidly dividing cells such as testis, ovary and small intestine (Amann et al., 1997). The function of ChlR1 during mitosis and its role in mammalian cells is unknown. During the course of experiments to determine the mechanism of chromosomal attachment of papillomavirus genomes during mitosis, mediated by the papillomavirus E2 protein, we identified several potential candidates using a yeast 2-hybrid screen to identify potential E2 binding proteins (Parish et al., 2007). In this manuscript we characterize the biology of one E2-interacting protein, ChlR1.

The *CHL1* (chromosome loss mutation) gene was first isolated in a screen in *Saccharomyces cerevisiae* for mutants exhibiting unusual mating phenotypes due loss of chromosome III, which carries mating type alleles (Haber, 1974; Liras et al., 1978). Deletion of *CHL1* caused a near 200-fold increase in the rate of chromosome III missegregation through both sister chromatid loss and sister chromatid non-disjunction, confirming a requirement for the 99 kDa protein it encodes, Chl1p, in the maintenance of correct chromosome transmission (Gerring et al., 1990). A functional ATP-binding motif is required for normal chromosome segregation since overexpression of Chl1p mutants that are defective for ATP binding interferes with high fidelity chromosome transmission (Holloway, 2000). Mutation of *CHL1* also results in a delay in the cell cycle at G_2/M (Gerring et al., 1990), although the mechanism of this remains unclear.

Human CHL1-related (ChlR1) encodes a protein with a predicted molecular mass of 102 kDa, and of unknown cellular function. The protein has 33% identity and 50% homology to Chl1p (Amann et al., 1997), although it is unclear whether ChlR1 is the true homologue of yeast Chl1p. The human DNA helicase BACH1 also has strong homology to Chl1p (24% identity and 42% homology) and it has been suggested that this may be the human homologue of Chl1p (Das and Sinha, 2005; Skibbens, 2004; Skibbens, 2005). However, BACH1 is necessary for DNA damage repair when in complex with the breast cancer susceptibility gene, *BRCA1* (Cantor et al., 2001) and *CHL1* mutations have no detectable defects in DNA repair (Gerring et al., 1990; Liras et al., 1978; Spencer et al., 1990), suggesting that Chl1p functionally differs from BACH1.

Recent studies have suggested a role for yeast Chl1p in the establishment of cohesion during S phase, either through a physical association with Ctf7p/Eco1p (Skibbens, 2004), or by interaction with components of the replication machinery (Mayer et al., 2004; Petronczki et al., 2004). Ctf7p/Eco1p is

necessary for the establishment of cohesion during DNA replication but is not directly involved in holding sister chromatids together (Skibbens et al., 1999; Toth et al., 1999). Ctf7p/Eco1p encodes an acetyltransferase that both acetylates itself and proteins within the cohesion complex in vitro (Ivanov et al., 2002). However, the role of acetyltransferase activity in Ctf7p/Eco1p function during cohesion establishment at S phase remains unresolved since acetylation-defective mutants are competent in high fidelity chromosome transmission (Brands and Skibbens, 2005). It is also shown that Ctf7p/Eco1p physically interacts with all three replication factor C (RFC) complexes, providing evidence that cohesion establishment is intimately linked to DNA replication (Kenna and Skibbens, 2003). Interestingly, deletion of both *CTF8*, a component of the RFC-Ctf18 complex, and *CHL1* results in abnormal sister chromatid cohesion (Mayer et al., 2004; Petronczki et al., 2004) adding further evidence that cohesion is linked to DNA replication and that Chl1p is required for this process. However the exact role of Chl1p in cohesion establishment remains to be determined.

Cohesion in mammalian cells is established by the protein complex cohesin, which consists of at least four proteins; Scc1 (Rad21), SA1/2, Smc1 and Smc3 (Uhlmann, 2004). These four subunits appear to form a ring structure that topologically holds sister chromatids together until anaphase onset (Gruber et al., 2003). Removal of cohesin from chromatin in mammalian cells is a two-step process, starting with removal from the arms of chromatid pairs prior to or very early in mitosis, followed by removal from centromeres at anaphase onset (Hoque and Ishikawa, 2001). Sister chromatid separation is triggered at anaphase by cleavage of Scc1 at the centromeric regions by the cysteine protease Separase (Uhlmann et al., 1999; Uhlmann et al., 2000). Separase is thought to act by specifically cleaving chromatin-bound Scc1 that has been hyperphosphorylated by Polo-like kinase 1 (Hoque and Ishikawa, 2001; Hornig and Uhlmann, 2004).

Here, we show that ChlR1 has a dynamic localization during mitosis. We characterize ChlR1 function and show that it binds cohesin and is required for normal sister chromatid cohesion. Depletion of ChlR1 results in abnormal sister chromatid cohesion and a delay at pro-metaphase. Mitotic failure then leads to genetic instability, an important step in cancer progression (Kops et al., 2005).

Results

Sub-cellular localization of ChlR1

Previous studies have shown by biochemical fractionation and indirect immunofluorescence methods (Holloway, 2000; Skibbens, 2004) that *S. cerevisiae* Chl1p is localized to the nucleus. Localization of ChlR1 in mammalian cells is less clear. To further characterize the localization of ChlR1, goat anti-peptide antibody to the C terminus of ChlR1 (2075) was produced (see Materials and Methods). This antiserum specifically immunoprecipitates radiolabeled FLAG-ChlR1 protein in vitro (Fig. 1A) and in vivo (Fig. 1B) with efficiency and specificity similar to the previously characterized Hel1 antiserum (Amann et al., 1997). We also confirmed immunoprecipitation of endogenous ChlR1 protein from cell lysates with our ChlR1 2075 antiserum, followed by western blot analysis with Hel1 (Fig. 1C). ChlR1 2075 does not detect ChlR1 protein by western blotting. This may indicate that the antibody specifically recognizes a conformational epitope in the native protein and therefore is predicted highly specific for immunoprecipitation and immunofluorescence techniques.

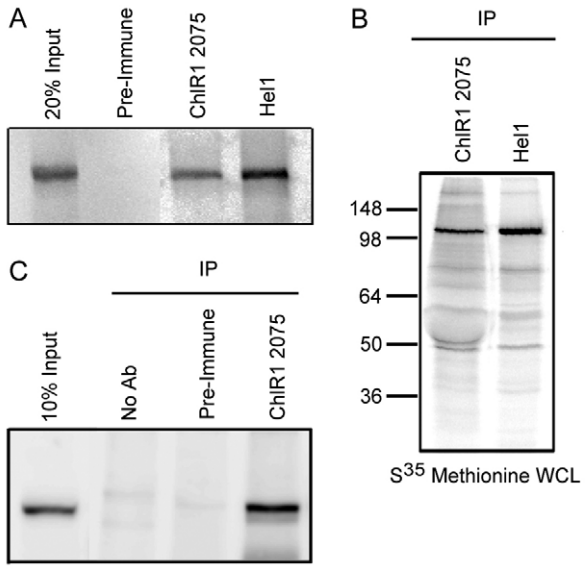

Fig. 1. Anti-peptide ChlR1 2075 antibody specifically immunoprecipitates ChlR1 protein. FLAG-ChlR1 was in vitro translated using a TNT kit (Promega) and the protein was used for immunoprecipitation with ChlR1 2075 or previously characterized Hel1 antibody (Amann et al., 1997). (B) Cells were transfected with FLAG-ChlR1 and metabolically radiolabeled. Whole cell lysate was used for immunoprecipitation with either ChlR1 2075 antisera or Hel1 (Amann et al., 1997). A band corresponding to the predicted molecular mass of ChlR1 (~102 kDa) was specifically immunoprecipitated with both antibodies. (C) HeLa cell lysates were used to immunoprecipitate endogenous ChlR1 protein with ChlR1 2075 antibody followed by detection by western analysis with the Hel1 antibody.

Diploid primary retinal epithelial cells immortalized by hTERT (RPE1) were synchronized by double-thymidine block then released to obtain a high proportion of mitotic cells. During the early stages of mitosis, ChlR1 localized to condensed chromatin (Fig. 2A) and released from the chromatin with progression to metaphase. ChlR1 was also localized to the spindle poles throughout mitosis and at the midbody at later stages of mitosis (Fig. 2A, metaphase to telophase). Some co-localization with α-tubulin staining on the spindle fibers was observed at metaphase (Fig. 2A and Fig. 3A). In late telophase, ChlR1 remained on the midbody and returned to the nuclear compartment. A similar pattern was observed with Hel1 antibody, thus confirming the localization of ChlR1; an identical pattern was seen in other cell types, including HeLa, Cos-7 and C33a cells (data not shown).

Immunofluorescence in unsynchronized cells showed nuclear localization with nucleolar exclusion in interphase cells (Fig. 2A), which was reproduced with affinity purified Hel1 antiserum (data not shown). Earlier studies showed that ChlR1 staining in interphase cells is localized to the nucleolus with nuclear exclusion (Amann et al., 1997). However, further analysis revealed that this localization was only observed with early bleeds of the Hel1 antibody, whereas later bleeds and affinity purified antibody had minimal nucleolar staining and

stronger nuclear staining, suggesting that the specificity of the antibody improved over time. To support this hypothesis, our unrelated goat anti-ChlR1 antibody shows similar staining patterns to the later bleeds of Hel1 antiserum at all stages in the cell cycle. Importantly the immunofluorescence signal was significantly reduced at all of the sites described above when ChlR1 expression was reduced with specific siRNAs (Fig. 2B and data not shown); control siRNAs did not affect ChlR1 localization. No specific staining was observed with pre-immune serum or when the 2075 antiserum was blocked with its cognate peptide (Fig. 2B).

In order to confirm the localization of ChlR1 at the spindle poles and midbody, cells were co-stained with antibodies to proteins that specifically localize to these structures. γ-tubulin is an essential component of the centrosomes (Stearns et al., 1991). Co-localization of ChlR1 with γ-tubulin was observed at all stages of mitosis, confirming association with the centrosomes and spindle poles, with ChlR1 staining also extending down the microtubule fibers (Fig. 3A and data not shown). To confirm ChlR1 localization to the midbody, cells were co-stained with Aurora B antibodies. Aurora B is a chromosomal passenger protein that has a dynamic localization during mitosis and localizes to the midbody at telophase (Murata-Hori et al., 2002). ChlR1 and Aurora B co-localized at later stages of mitosis (Fig. 3B), confirming our observation that ChlR1 localizes to the midbody at telophase.

Depletion of ChlR1 results in a pro-metaphase delay and subsequent mitotic failure

It has been reported that there is a delay in G_2/M phase of the cell cycle in *CHL1*-null *S. cerevisiae* (Gerring et al., 1990). To test the requirement for ChlR1 during mitotic progression, a tetracycline-inducible RNA interference system was established (see Materials and Methods). The shRNA target sequence used to deplete ChlR1 was used to extensively search public databases for similarity to other known mRNA sequences. No sequence similarity with other mRNA sequences was detected, including the closely related BACH1 mRNA sequence. Doxycycline treatment of these cells induced expression of the ChlR1-specific shRNA and effectively depleted ChlR1 RNA and protein by ~60% (Fig. 4A,B); induction of control shRNA cells had no effect on ChlR1 protein levels. Removal of doxycycline from the growth medium restored ChlR1 to normal levels (data not shown).

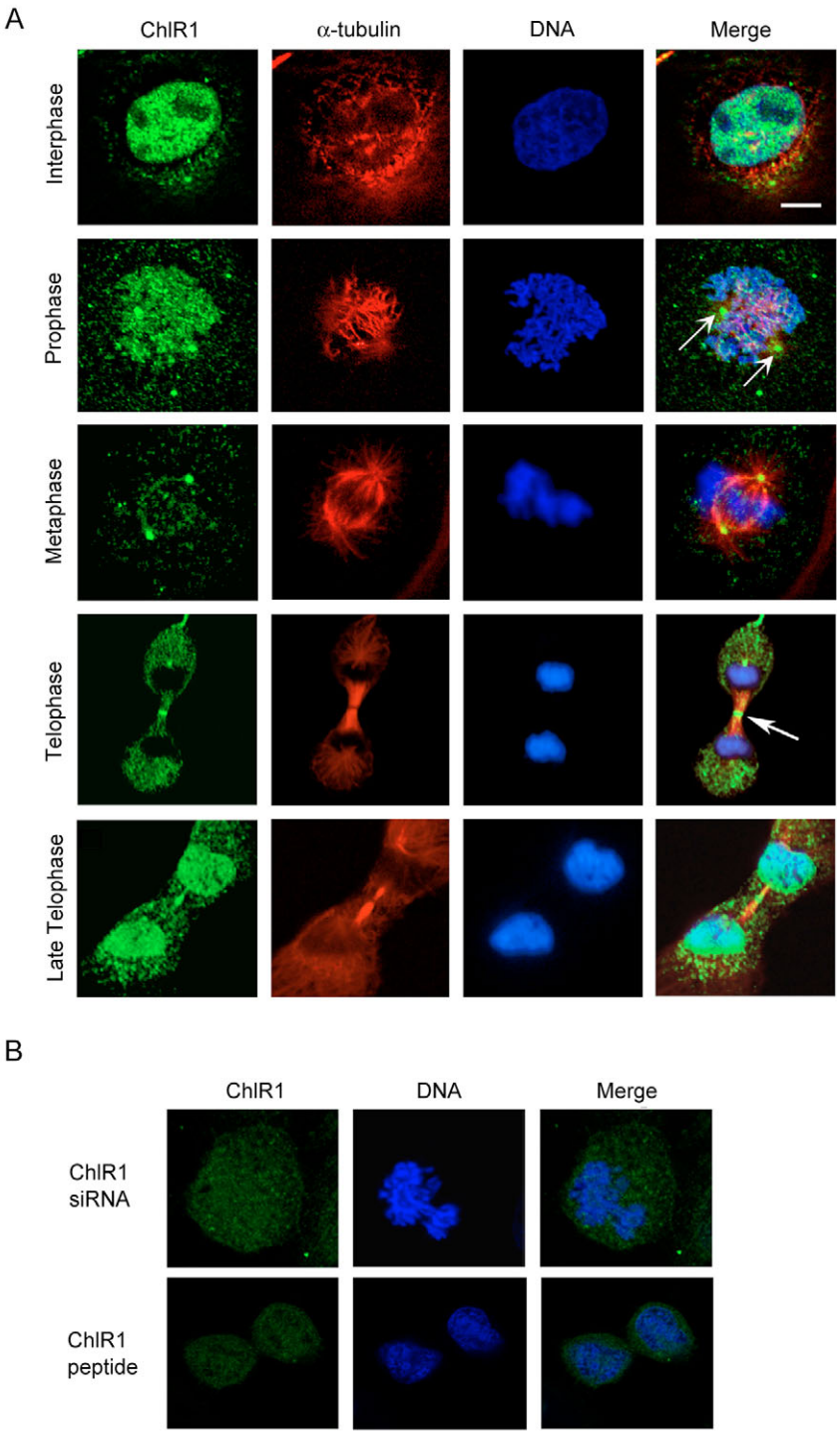

Fig. 2. ChlR1 localizes to chromatin, spindle poles and the midbody. Confocal images of ChlR1 localization in RPE-1 cells at different stages of mitosis. (A) ChlR1 was detected using antibody 2075 (green), α-tubulin was stained red and DNA stained blue; merged images are shown on the right. Bar, 8 μm. Spindle poles and midbody structures are indicated by arrows in prophase and telophase, respectively. (B) Top panels: RPE1 cells were transfected with 20 nM ChlR1-specific siRNA and stained for ChlR1 protein (green) and DNA (blue). Image shown is a cell at metaphase with no detectable ChlR1-specific staining at the spindles poles. Bottom panels: ChlR1 2075 antibody was incubated with 50 μg/ml ChlR1 peptide (used to raise antibody) for 15 minutes at room temperature and then used to detect ChlR1 in RPE1 cells. Incubation of ChlR1 antiserum with peptide significantly reduced specific fluorescence (a telophase cell is shown).

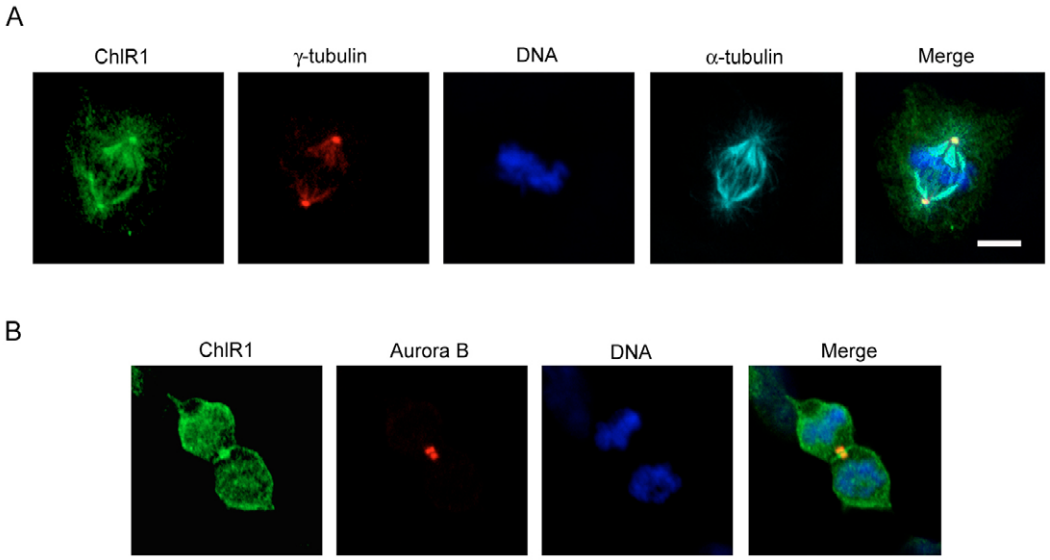

Fig. 3. ChlR1 co-localizes with γ-tubulin and Aurora B at the centrosomes and midbody, respectively. RPE1 cells were fixed as previously described and stained for (A) ChlR1 (green), γ-tubulin (red), α-tubulin (cyan) and DNA (blue) in metaphase, and (B) ChlR1 (green), Aurora B (red) and DNA blue in telophase; merged images are shown on the right. Bar, 8 μm for all parts of the figure.

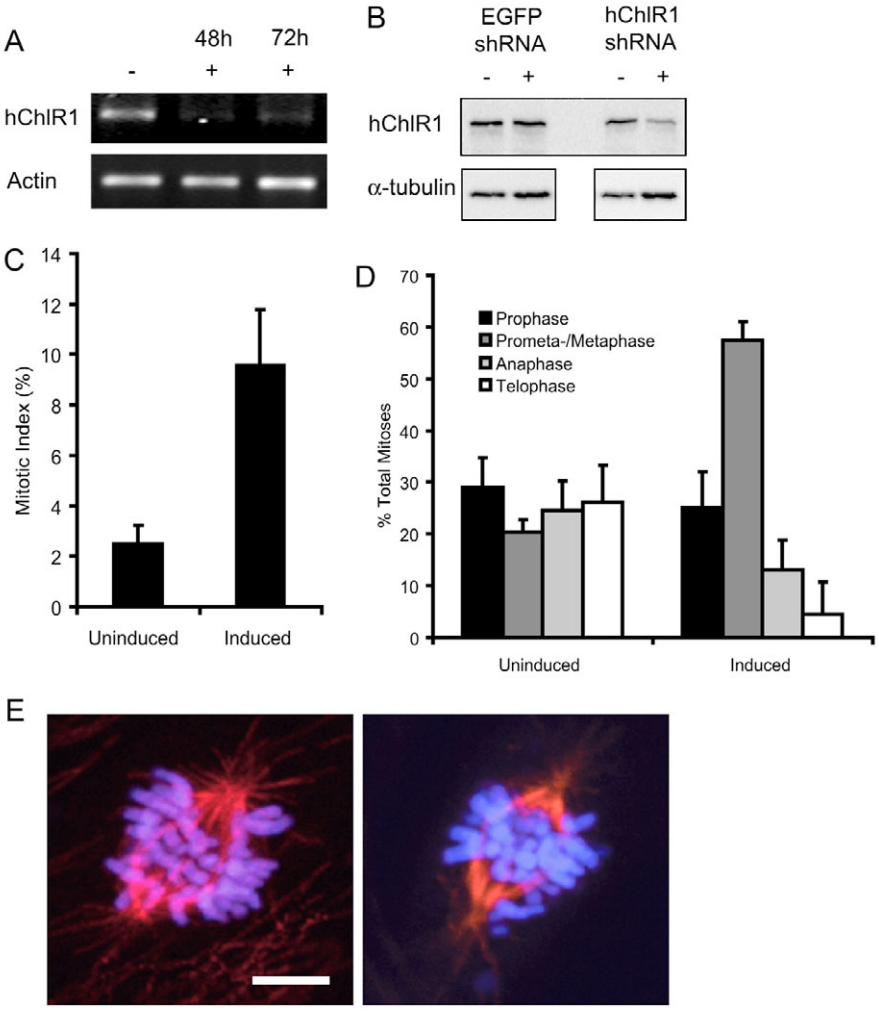

Fig. 4. shRNA-mediated depletion of ChlR1 results in mitotic delay. (A) RT-PCR results with ChlR1-specific (top panel) or actin-specific (lower panel) primers from DNase-treated RNA purified from RPE1-TetR-ChlR1 cells with shRNA expression uninduced or induced at 48 and 72 hours with 2 μg/ml doxycycline. (B) ChlR1 (upper panel) and α-tubulin (lower panel) protein levels in RPE1-TetR-EGFP cells or RPE1-TetR-ChlR1 cells with uninduced and induced shRNA for 24 hours with 2 μg/ml doxycycline. (C) RPE1-TetR-ChlR1 cells were grown on coverslips and ChlR1 shRNA was uninduced or induced for 24 hours with 2 μg/ml doxycycline before cells were pre-extracted with 0.1% Triton X-100 and fixed in methanol. Mitotic cells were stained for α-tubulin (red) by indirect immunofluorescence and for DNA (blue) using Hoechst no. 33568. More than100 cells were counted per experiment and the mean percentage of mitotic cells for three independent experiements determined and expressed as the mitotic index (± s.d.). (D) More than 50 mitotic cells per experiment were assessed for specific mitotic stage and the percentage of total mitoses for three independent experiments calculated (± s.d.). An increase in pro-metaphase cells with concomitant decrease in other mitotic stages was observed following depletion of ChlR1. Shown is the mean and standard deviation of at least three independent experiments. (E) Representative confocal images of RPE1-TetR-ChlR1 cells with ChlR1 shRNA induced for 24 hours; α-tubulin was stained red and DNA stained blue. Bar, 8 μm.

Detailed examination of cellular morphology following induction of ChlR1-specific shRNA revealed an increase in the percentage of mitotic cells at 24 hours (Fig. 4C). Close inspection of the mitotic population revealed a significantly higher percentage of cells with chromosomes dispersed over the entire spindle, a phenotype characteristic of pro-metaphase (Fig. 4D,E). In addition, there was a concomitant decrease in the percentage of cells in other mitotic stages (Fig. 4D), indicating an arrest at pro-metaphase. In order to determine whether cells with lower levels of ChlR1 protein would overcome the observed pro-metaphase arrest, cells were incubated in the presence of doxycycline for 96 hours. This resulted in the formation of cells with enlarged and fragmented nuclei in comparison to uninduced cells (Fig. 5A,B), indicating that ChlR1-depleted cells fail to correctly segregate sister chromatids following delay at pro-metaphase. Nuclear abnormalities resulting from depletion of ChlR1 protein were observed in over 25% of cells compared to 2% observed in the uninduced cells (Fig. 5C).

To identify the mechanism of mitotic failure following ChlR1 depletion, we transfected HeLa cells with siRNAs that targeted the same region of ChlR1 as the inducible shRNAs. Western blotting showed that ChlR1 protein was specifically depleted by ~95% compared to controls (Fig. 6A). As with RPE1 cells, HeLa cells depleted of ChlR1 had an increase in the mitotic index due to accumulation in pro-metaphase and a concomitant decrease in other mitotic stages (data not shown). Time-lapse imaging of cells stained with Syto13 to label chromatin revealed a failure to form a tight metaphase plate compared to control cells (Fig. 6B,C). In cells imaged following ChlR1 depletion, chromosomes moved

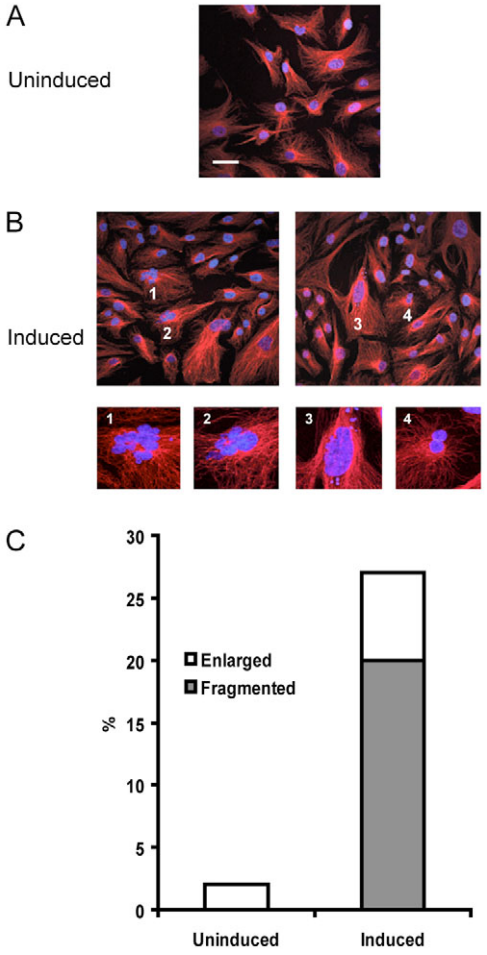

Fig. 5. ChlR1 depletion results in mitotic failure. (A) Normal nuclear morphology in uninduced RPE1-TetR-ChlR1 cells (B) RPE1-TetR-ChlR1 cells were induced with 2 μg/ml doxycycline for 96 hours. Representative nuclear abnormalities are indicated (1-4) and enlargements are shown below. α-Tubulin was stained red and DNA stained blue. Bar, 40 μm except for enlargements. (C) Quantification of nuclear abnormalities before and after induction of ChlR1 shRNA. Cells within a field of view were counted and the percentage of nuclear abnormalities determined and classified as fragmented (grey) or abnormally large (white). Data are the average of ten fields of view for each sample.

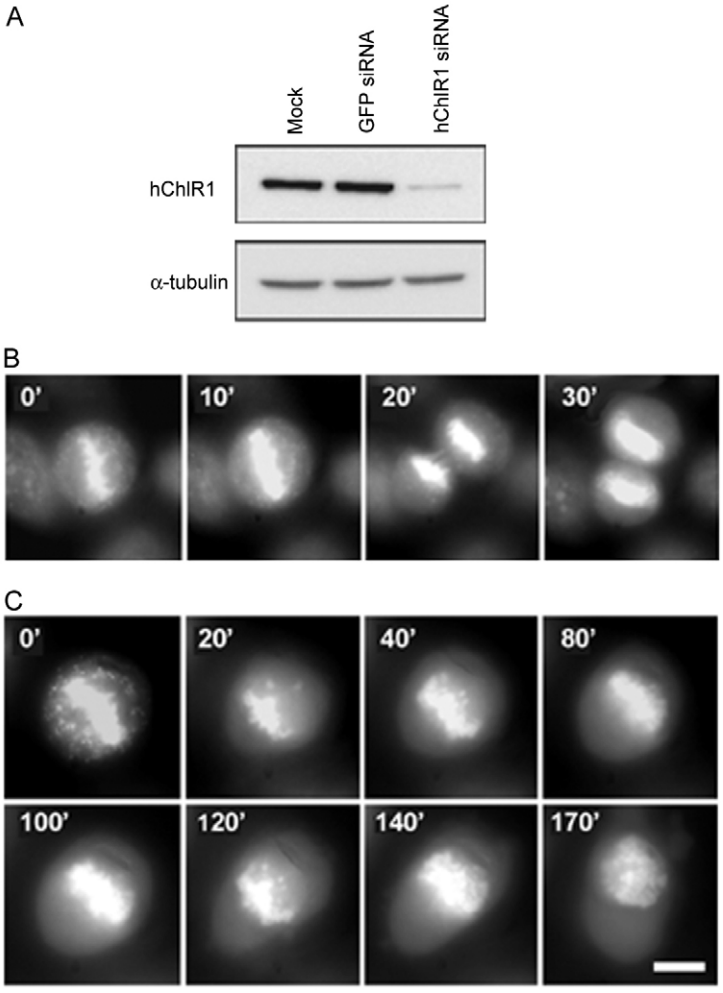

Fig. 6. ChlR1 depletion results in mitotic delay and failure. HeLa cells were transfected with siRNA duplexes specific for ChlR1, or GFP as a control. (A) 24 hours following transfection, cells were harvested for western analysis of ChlR1 protein expression using Hel1 antibody. α-Tubulin was included as a loading control. Control (B) or ChlR1 siRNA-transfected (C) cells were stained with 1 μM Syto13 to label DNA and filmed by time-lapse imaging using a 20× objective and a TRITC filter set. Numbers in upper left of each panel indicate minutes after start of filming. Bar, 10 μm.

bidirectionally on mitotic spindles similar to pro-metaphase cells but were unable to establish a stable metaphase configuration. After approximately 3 hours in the pro-metaphase-like state, the DNA eventually decondensed without mitotic segregation. Multiple cells (n=6) were filmed following transfection with ChlR1-specific siRNA and all failed to enter anaphase and complete mitosis normally.

ChlR1 associates with the cohesion complex in vivo

Recent data indicate that in yeast Chl1p functions in cohesion establishment via direct or indirect interaction with proteins required for cohesion establishment (Mayer et al., 2004; Petronczki et al., 2004; Skibbens, 2004). Even though the proteins isolated in these studies were not the cohesin subunits per se, we sought to determine whether ChlR1 plays a central role in cohesion establishment in mammalian cells by associating with the cohesin complex. HeLa cell lysates were used to immunoprecipitate ChlR1-containing protein complexes with ChlR1-specific (2075) antisera, and co-precipitating cohesin subunits Scc1, Smc1 and Smc3 were reproducibly co-immunoprecipitated (Fig. 7A). Since this immunoprecipitation experiment was performed using endogenously expressed proteins, it is probably a physiological association. In order to confirm the specificity of cohesin co-precipitation with ChlR1-specific antibodies, ChlR1 protein levels were depleted by transfection of cells with ChlR1 or GFP-specific siRNAs. Scc1 was co-precipitated from lysates of untransfected or GFP siRNA-transfected cells, but depletion of ChlR1 protein resulted in a significant reduction of Scc1 protein co-precipitating with ChlR1 antisera (Fig. 7B), indicating specificity of the co-immonuprecipitation assay. Co-immunoprecipitation of Scc1, Smc1 and Smc3 with ChlR1 was also confirmed using with Hel1 antisera (data not shown). Although a direct interaction of ChlR1 with cohesin subunits cannot be resolved using this assay, ChlR1 is clearly in complex with the cohesin complex. Interestingly, association with the cohesin subunit hSA1/2 was not observed (Fig. 7A), suggesting the presence of a unique complex lacking the hSA1/2 subunit.

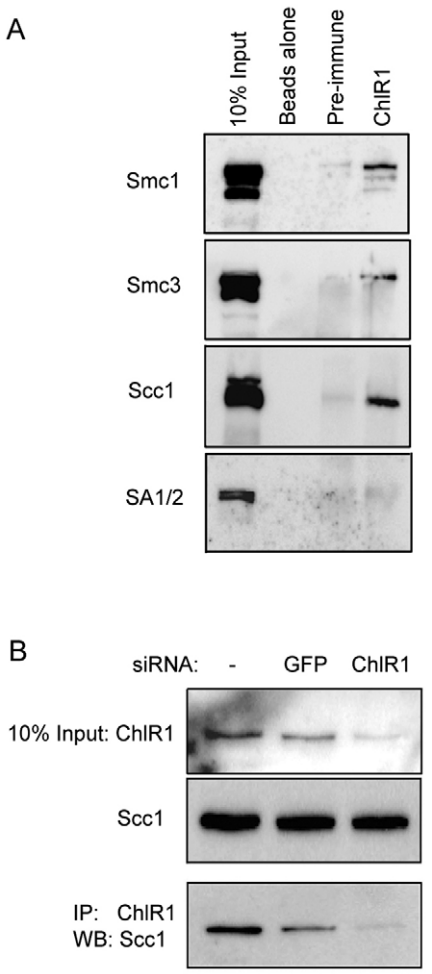

Fig. 7. Mammalian cohesin co-immunoprecipitates with ChlR1. HeLa cell lysates were incubated with protein G beads alone or in combination with pre-immune serum or ChlR1 2075 antibody as indicated at the top of the immunoblots. Specific interaction with components of the cohesin complex was detected by western blotting using antibodies to Smc1, Smc3, Scc1 or SA1/2 as indicated on the left. (B) To confirm specificity of the interaction, cells were transfected with 20 nM siRNAs as indicated at the top of the immunoblots. ChlR1 protein levels were efficiently reduced following transfection with specific siRNA but not with GFP control. Scc1 input is shown to be unaltered (middle panel). Depletion of ChlR1 protein levels results in a proportional decrease in the amount of co-immunoprecipitating Scc1 protein compared to controls (lower panel).

Depletion of ChlR1 results in cohesion abnormalities

Mutation of *CHL1* in *S. cerevisiae* resulted in abnormal cohesion establishment as demonstrated by precocious separation of a URA3 locus marker before the onset of anaphase and by the accumulation of cells in metaphase (Petronczki et al., 2004). In view of our observation that ChlR1 depletion in mammalian cells causes abnormalities in mitotic progression and that ChlR1 associates with the cohesion complex, we tested whether ChlR1 depletion would cause physical abnormalities in sister chromatid cohesion. HeLa cells were transfected with ChlR1-specific siRNAs and sister chromatid pairing was visualized in metaphase spreads. Control transfected cells showed normal chromatid pairing with a tight association between pairs. However, depletion of ChlR1 protein resulted in chromatids that appeared to be loosely paired (Fig. 8A). Measurement of the distance between chromatid pairs revealed that associated sister chromatids were significantly further apart at the centromeric region. The spacing between chromatid pairs was increased from an average of 1.6 μm in controls to 2.5 μm after ChlR1 depletion (P<0.0002) (Fig. 8B), strongly indicating abnormalities in sister chromatid cohesion.

Discussion

This is the first report of ChlR1 function during mitosis and provides the basis for several avenues of research. The mitotic locations of ChlR1 provide important insights into the functions of the protein. Its association with mitotic chromatin in prophase and into pro-metaphase suggests that ATP-dependent DNA helicase activity is required for chromatin condensation and organization of DNA. Mammalian cohesin is associated along the length of the chromatin very early in mitosis, but translocates from the chromosome arms as the

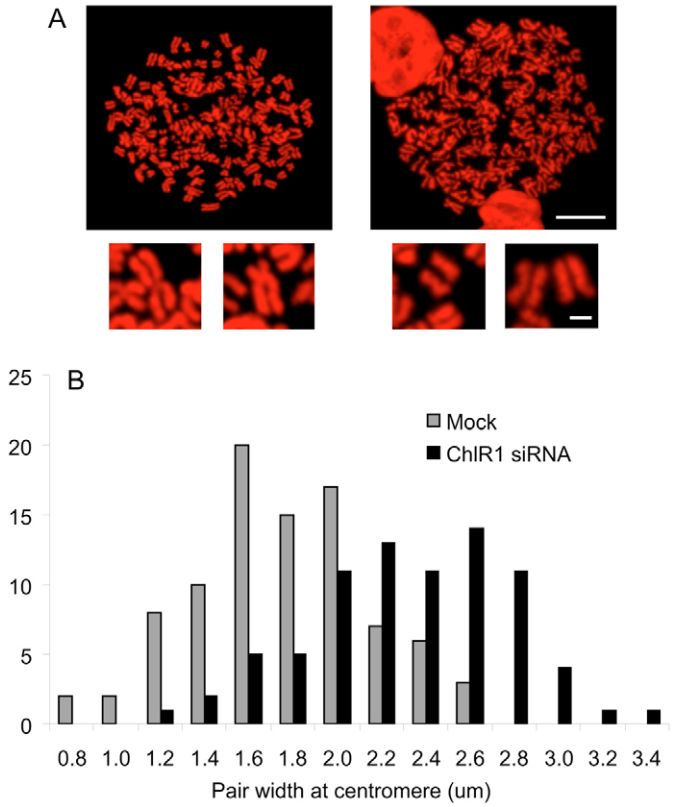

Fig. 8. Depletion of ChlR1 results in abnormal sister chromatid cohesion. (A) HeLa cells were untransfected (left) or transfected with ChlR1-specific siRNA (right) and metaphase spreads prepared 24 hours following transfection. DNA was stained with propidium iodide and chromosome morphology visualized by confocal microscopy. Bar is 8 μm in top images and 1 μm in enlargements shown underneath. (B) The distance between chromatid pairs was measured using Leica confocal software of at least ten images taken from untransfected (grey) and ChlR1-specific siRNA (black) transfected cells. The graph shows distribution of pair width for each data set. The difference between mock and transfected cells was statistically analyzed using Student's *t*-test; $P<0.0002$.

cells progress into pro-metaphase (Watanabe, 2005) with similar dynamics to the loss of ChlR1 on the chromatid arms at pro-metaphase. In light of the association of ChlR1 with components of the cohesin complex and abnormal sister chromatid cohesion following ChlR1 depletion, we propose that ChlR1 is required for the correct assembly of cohesin onto DNA during replication (S-phase) and is removed from the chromatid arms along with cohesin early in mitosis. Interestingly, ChlR1 localization is not observed at centromeric regions during metaphase where cohesin remains (Waizenegger et al., 2000) implying the helicase does not function as a structural cohesion protein during chromosome congression.

When ChlR1 protein levels are reduced, an increase in pro-metaphase arrested cells is observed. This may indicate that the Mad2-dependent spindle checkpoint is activated, preventing anaphase onset. This would cause a delay at pro-metaphase, presumably by inhibiting spindle attachment to kinetochores. Immunoflourescent staining of pro-metaphase-arrested cells with kinetochore markers such as CENP-E, BubR1 and Bub1 following depletion of ChlR1 does not clearly show unpaired chromosomes that could activate the checkpoint. Therefore, it is more likely that depletion of ChlR1 results in abnormal kinetochore assembly and function. Interestingly, it has been shown that depletion of Scc1 by RNAi results in a dramatic increase in mitotic cells specifically delayed at pro-metaphase, and is associated with abnormal cohesion establishment (Sonoda et al., 2001; Vass et al., 2003). Scc1-depleted cells exhibited abnormal kinetochore assembly with mislocalization of the chromosomal passenger inner centromeric protein (INCENP) from the normal discrete association with the inner centromeric regions to a more diffuse localization on the chromatids, presumably because the chromatids are no longer in proximity (Sonoda et al., 2001; Vass et al., 2003). The role of ChlR1 in kinetochore assembly is currently under investigation, but it is enticing to speculate that ChlR1-dependent cohesion establishment directly affects kinetochore assembly and function such that chromatids with insufficient cohesion cannot capture mitotic spindles correctly to satisfy the spindle checkpoint and progress to anaphase.

Recently, an essential role of helicases in the establishment of cohesion has been proposed and a specific role for *S. cerevisiae* Chl1p in the unwinding of cohesin-chromatin complexes has been suggested (Skibbens, 2005). Along with the emerging function of Chl1p, other DNA helicases have been implicated in the establishment of cohesion. A screen for proteins involved in chromatid cohesion revealed three DNA helicases that participate in cohesion: Sgs1p, Rrm3p and Srs2p (Warren et al., 2004). Human homologues of these helicases include the BACH1 and WRN helicases. Interestingly, mutations in these helicases result in abrogation of the G_2 decatenation checkpoint (Deming et al., 2001; Franchitto et al., 2003), although it been suggested that a defect in cohesion is more probably the cause of the chromosomal abnormalities observed in these cells, as gaps between sister chromatids in metaphase spreads have been observed (Deming et al., 2001; Skibbens, 2005).

The immunofluorescence data presented here show that ChlR1 is concentrated at the spindle poles at very early stages of mitosis and remains associated with these structures into telophase. The cohesion subunits Smc1 and SA1 have been shown to localize to the spindle poles during mitosis via an interaction with NuMA, a protein required for mitotic spindle organization (Gregson et al., 2001). Furthermore, the same study found that depletion of cohesin subunits in HeLa mitotic extracts inhibited mitotic aster assembly. It has also been reported that depletion of the Scc1 homologue in *Drosophila* results in a failure of sister chromatid cohesion in conjunction with abnormally narrow spindles without astral assembly (Vass et al., 2003). Taken together, these data suggest a new role for cohesin following sister chromatid cohesion establishment. Interestingly, another ATP-dependent DNA helicase, RUVBL1/TIP49a, was reported to be concentrated at the centrosomes and associate with mitotic spindles during early stages of mitosis (Gartner et al., 2003). RUVBL1 is essential for cellular division and proliferation (Lim et al., 2000), and it is suggested that this protein plays a role in microtubule organization during mitosis since it directly associates with α- and γ-tubulin and was shown to increase tubulin polymerization when over-expressed in the presence of Paclitaxel, a microtubule stabilizer (Gartner et al., 2003). The

localization of ChlR1 at the spindle poles in addition to its association with cohesin may indicate a role for ChlR1 in spindle aster assembly, although no spindle morphology defects were observed following ChlR1 depletion in the course of this study.

During cleavage furrow ingression, ChlR1 is concentrated at the midbody and remains associated with the spindle poles. At late-stage telophase, ChlR1 is concentrated within the newly formed nucleus, suggesting that either ChlR1 is transported back into the nuclear compartment or protein synthesis is initiated as soon as the nuclear envelope reforms. Localization of ChlR1 at the midbody is intriguing and it remains to be determined whether ChlR1 has a specific function within the midbody or if ChlR1 mediates another activity during cytokinesis.

In this paper we provide evidence that a DNA helicase is directly involved in sister chromatid cohesion. Knockdown of ChlR1 results in abnormal sister chromatid cohesion and this causes defects during early mitosis and eventually mitotic failure resulting in the development of aneuploid cells. Aneuploidy is one of the most common features of tumors. Differences in chromosome number from cell to cell within the same tumor are common, indicating that tumor cells have systemic abnormalities with mitotic segregation and cytokinesis, or the checkpoints that control mitosis are not intact (Rajagopalan and Lengauer, 2004). It will be important to determine if changes in ChlR1 expression or stability in vivo leads to chromosomal instability and hence tumorigenesis.

Materials and Methods

Plasmids

pcDNA6/TR (a gift from F. Yao, Harvard Medical School, MA) expresses the tetracycline repressor protein (tetR) from a CMV promoter. pcDNA4/TO-luciferase (a gift from H. Clevers, Netherlands Cancer Institute, Amsterdam) expresses Firefly luciferase under the control of a CMV promoter containing tetR DNA binding sites. The plasmid pSuperior-puro (Oligoengine, Seattle, WA) was used to express shRNA molecules from a tetracycline-inducible H1 promoter. Annealed oligonucleotides (5′-gatccccgacttcatggcagagctgtttcaagagaacagctctgccatgaagtcttttt-3′ and 5′-agctaaaagacttcatggcagagctgttctcttgaaacagctctgccatgaagtcggg-3′ for ChlR1 shRNA and 5′-gatccccgctgaccctgaagttcatcttcaagagagatgaacttcagggtcagctttt-3′ and 5′-agctaaaagctgaccctgaagttcatctctcttgaagatgaacttcagggtcagcggg-3′ for EGFP shRNA) were ligated into pSuperior-puro to produce pSuperior-puro-ChlR1 and pSuperior-puro-EGFP, respectively. pCMV-FLAG-ChlR1 expresses FLAG-ChlR1 from a CMV promoter.

Antibodies

Affinity purified Hel1 antisera was raised to amino acids 2-130 of ChlR1 (Amann et al., 1997). Goat anti-ChlR1 2075 antoserum was raised against amino acids 893-906 of ChlR1 (AAVQKFHREKSASS) and affinity purified using the MicroLink™ peptide coupling kit (Pierce). γ-tubulin antibodies were raised in rabbit against peptide AATRPDYISWGTQDK. Antisera specific to Smc1, Smc3, Scc1/Rad21 and SA1/2 were a gift from K. Yokomori, Howard Hughes Medical Institute, University of California, Irvine, CA (Gregson et al., 2001). Aurora B antibodies (Aim-1) were purchased from BD Biosciences. For immunofluorescence, chicken anti-mouse Alexa Fluor 647, donkey anti-rabbit Alexa Fluor 633 and donkey anti-goat Alexa Fluor 488 1gGs (Molecular Probes) were diluted 1:1000. Zenon Alexa Fluor 546 mouse IgG_1 (Molecular Probes) was used to stain α-tubulin.

Cell culture

HeLa cells were maintained in Dulbecco's minimal essential medium, supplemented with 10% fetal bovine serum, 100 units/ml penicillin and 100 μg/ml streptomycin. RPE1 cells (Clontech) were maintained in Dulbecco's minimal essential medium and Ham's F12 medium (50:50) supplemented with 10% fetal bovine serum, 100 units/ml penicillin and 100 μg/ml streptomycin.

Metabolic radiolabeling of cells

HeLa cells transfected with pCMV-FLAG-ChlR1 were incubated in Met-/Cys-DMEM supplemented with 10% dialyzed FBS for 1 hour before adding 200 μCi/ml [^{35}S]methionine to the medium. Cells were incubated in the presence of the radioisotope for 24 hours at 37°C. Whole cell lysates were then used in immunoprecipitation experiments.

Immunofluorescence and confocal imaging

Cells were grown on acid-washed poly-L-lysine (Sigma)-treated coverslips and pre-extracted in preperm buffer (80 mM Pipes, 5 mM EGTA, 1 mM $MgCl_2$, 0.1% Triton X-100, v/v, pH 6.8) for 30 seconds before incubation in fixing buffer (80 mM Pipes, 5 mM EGTA, 1 mM $MgCl_2$, 3.7% paraformaldehyde, pH 6.8) for 1 minute, at room temperature. Cells were then fixed in methanol for 30 minutes at –20°C and washed in 2× PBS before incubation in PBS-AT (1× PBS, 1% BSA w/v, 0.05% Triton X-100 v/v) for 30 minutes at room temperature. To stain DNA, cells were incubated with Hoechst No. 34580 (5 μg/ml in PBS) at room temperature for 10 minutes and then washed 4× 10 minutes with PBS before inverting coverslips onto Fluoromount G (Southern Biotechnology Associates, Inc., Birmingham, AL). Images were collected using a Leica TSC SP2 AOBS confocal microscope and processed using Leica Imaging software.

Inducible shRNA

RPE1 cells were transfected with pcDNA6/TR and individual clones isolated after selection in 5 μg/ml blasticidin S HCl (Invitrogen) for 3 weeks. Clones were transfected with 50 ng pcDNATO/Luc in a 6-well plate and incubated for a further 24 hours in the presence or absence of doxycycline (Sigma). Cells were then lysed in Luciferase lysis buffer (Promega) and activity determined using a Firefly Luciferase assay kit (Promega). The induction of luciferase expression upon addition of doxycycline to the growth medium was tested for numerous clones isolated. The best clone in this assay was then transfected with pSuperior-puro-ChlR1 or pSuperior-puro-EGFP, to make RPE1-TetR-ChlR1 and RPE1-TetR-EGFP, respectively, and a polyclonal stable population was established. shRNA expression was then induced with 2 μg/ml doxycycline for 24-96 hours and specific knockdown determined both by RT-PCR and western analysis.

siRNA

siRNAs targeting ChlR1 and GFP mRNAs were made as complimentary single-stranded 19 mer siRNAs with 3′ dTdT overhangs (Qiagen), annealed and delivered into cells at a final concentration of 20 nM using Dharmafect 1 (Dharmacon, Inc., Lafayette, CO). The nucleotides targeted were as follows: in ChlR1, 212-229 and in GFP, 123-140.

RT-PCR

RNA was purified using an RNeasy mini kit (Qiagen) and treated with 1 μg DNase I (Promega). cDNA was then amplified using 200 units Superscript II (Invitrogen) and 20 pmoles oligonucleotide $(N)_6$ as detailed in the manufacturer's instructions. ChlR1 cDNA was amplified by PCR from 2 μl of cDNA, using primers 5′-gtgctaggggggaacattaagcaaa-3′ and 5′-gcgacccacctcgtccatcatctga-3′ by incubation at 94°C for 2 minutes followed by 30 cycles 94°C for 30 seconds, 56°C for 30 seconds and 72°C for 30 seconds. Actin cDNA was amplified from 1 μl cDNA by PCR using primers 5′-cacagtgctgtctggcggcaccac-3′ and 5′-aggatggcaagggacttcctgtaaca-3′ and 20 cycles of the PCR conditions described above.

Time-lapse imaging

HeLa cells were used for time-lapse imaging as they are much less sensitive to the viable dyes used for DNA imaging and light exposure from the live cell imaging process than RPE1 cells. Cells were grown on glass coverslips and stained with 1 μM Syto13 (Molecular Probes) for 10 minutes at 37°C, before fresh medium was added and the coverslip mounted onto a glass slide to create a sealed chamber. Cells were imaged in a heated chamber (37°C) every 10 minutes for 3-5 hours using a 20× phase-contrast objective and a TRITC filter set for Syto13-stained cells on an inverted microscope (Olympus IX-70). Images were captured on a CoolSnap HQ CCD camera (Roper Scientific, Tucson, AZ) and concatenated using Metamorph software (Universal Imaging Corp., Downington, PA).

Immunoprecipitations

Cells were grown in a 100 mm dish and lysed in 500 μl lysis buffer [50 mM Tris-HCl, pH 8.0, 100 mM NaCl, 20 mM NaF, 10 mM KH_2PO_4, 1% Triton X-100, 0.1 mM DTT, 10% glycerol and protease inhibitor cocktail tablet (Roche)]. Lysates were cleared by centrifugation and then 250 μl mixed 50:50 with binding buffer (50 mM Tris-HCl, pH 8.0, 100 mM KCl, 0.1 mM EDTA, 0.2% NP-40, 0.1% BSA, 2.5% glycerol, 2 mM DTT and protease inhibitor cocktail). 15 μl of protein G slurry (Amersham) was added to each sample and 1 μl of ChlR1 2075 or pre-immune serum added. Samples were incubated at 4°C for 4 hours with constant agitation and washed 4× 500 μl wash buffer (100 mM Tris-HCl, pH 8.0, 150 mM NaCl, 0.5% NP-40, 2 mM DTT). Remaining proteins were then separated by SDS-PAGE and co-immunoprecipitating proteins detected by western blot analysis.

Chromosomal spreads

HeLa cells were transfected with siRNA oligos specific for either ChlR1 or GFP mRNA and incubated for 24 hours. Cells were then blocked with 100 ng/ml colchicine for 2 hours and swelled in hypotonic buffer (0.8% sodium citrate) for 10

minutes at room temperature. Cells were fixed in Carnoy's fixative (75% methanol, 25% acetic acid) and spreads prepared by dropping suspended cells onto slides warmed to 37°C. Slides were then stained with 1 mg/ml propidium iodide in PBS and mounted in fluoromount G.

We thank Kyoko Yokomori and Hans Clevers for antibodies and plasmid constructs. We also thank Suzanne Melanson, Angela Bean and Yuval Bibi Nitzan for scientific discussion and critical reading of the manuscript, and Theodore Giehl for technical assistance with confocal microscopy. This work was supported by the National Institutes of Health grants R01 CA58376 to E.A., R01 GM51994 and CA82834 to S.D., and by the Department of Defense (PC030931) to S.D.

References

Amann, J., Kidd, V. J. and Lahti, J. M. (1997). Characterization of putative human homologues of the yeast chromosome transmission fidelity gene, CHL1. *J. Biol. Chem.* **272**, 3823-3832.

Brands, A. and Skibbens, R. V. (2005). Ctf7p/Eco1p exhibits acetyltransferase activity – but does it matter? *Curr. Biol.* **15**, R50-R51.

Cantor, S. B., Bell, D. W., Ganesan, S., Kass, E. M., Drapkin, R., Grossman, S., Wahrer, D. C., Sgroi, D. C., Lane, W. S., Haber, D. A. et al. (2001). BACH1, a novel helicase-like protein, interacts directly with BRCA1 and contributes to its DNA repair function. *Cell* **105**, 149-160.

Das, S. P. and Sinha, P. (2005). The budding yeast protein Chl1p has a role in transcriptional silencing, rDNA recombination, and aging. *Biochem. Biophys. Res. Commun.* **337**, 167-172.

Deming, P. B., Cistulli, C. A., Zhao, H., Graves, P. R., Piwnica-Worms, H., Paules, R. S., Downes, C. S. and Kaufmann, W. K. (2001). The human decatenation checkpoint. *Proc. Natl. Acad. Sci. USA* **98**, 12044-12049.

Franchitto, A., Oshima, J. and Pichierri, P. (2003). The G2-phase decatenation checkpoint is defective in Werner syndrome cells. *Cancer Res.* **63**, 3289-3295.

Gartner, W., Rossbacher, J., Zierhut, B., Daneva, T., Base, W., Weissel, M., Waldhausl, W., Pasternack, M. S. and Wagner, L. (2003). The ATP-dependent helicase RUVBL1/TIP49a associates with tubulin during mitosis. *Cell Motil. Cytoskeleton* **56**, 79-93.

Gerring, S. L., Spencer, F. and Hieter, P. (1990). The CHL 1 (CTF 1) gene product of Saccharomyces cerevisiae is important for chromosome transmission and normal cell cycle progression in G2/M. *EMBO J.* **9**, 4347-4358.

Gregson, H. C., Schmiesing, J. A., Kim, J. S., Kobayashi, T., Zhou, S. and Yokomori, K. (2001). A potential role for human cohesin in mitotic spindle aster assembly. *J. Biol. Chem.* **276**, 47575-47582.

Gruber, S., Haering, C. H. and Nasmyth, K. (2003). Chromosomal cohesin forms a ring. *Cell* **112**, 765-777.

Haber, J. E. (1974). Bisexual mating behavior in a diploid of Saccharomyces cerevisiae: evidence for genetically controlled non-random chromosome loss during vegetative growth. *Genetics* **78**, 843-858.

Hirota, Y. and Lahti, J. M. (2000). Characterization of the enzymatic activity of hChlR1, a novel human DNA helicase. *Nucleic Acids Res.* **28**, 917-924.

Holloway, S. L. (2000). CHL1 is a nuclear protein with an essential ATP binding site that exhibits a size-dependent effect on chromosome segregation. *Nucleic Acids Res.* **28**, 3056-3064.

Hoque, M. T. and Ishikawa, F. (2001). Human chromatid cohesin component hRad21 is phosphorylated in M phase and associated with metaphase centromeres. *J. Biol. Chem.* **276**, 5059-5067.

Hornig, N. C. and Uhlmann, F. (2004). Preferential cleavage of chromatin-bound cohesin after targeted phosphorylation by Polo-like kinase. *EMBO J.* **23**, 3144-3153.

Ivanov, D., Schleiffer, A., Eisenhaber, F., Mechtler, K., Haering, C. H. and Nasmyth, K. (2002). Eco1 is a novel acetyltransferase that can acetylate proteins involved in cohesion. *Curr. Biol.* **12**, 323-328.

Kenna, M. A. and Skibbens, R. V. (2003). Mechanical link between cohesion establishment and DNA replication: Ctf7p/Eco1p, a cohesion establishment factor, associates with three different replication factor C complexes. *Mol. Cell. Biol.* **23**, 2999-3007.

Kops, G. J., Weaver, B. A. and Cleveland, D. W. (2005). On the road to cancer: aneuploidy and the mitotic checkpoint. *Nat. Rev. Cancer* **5**, 773-785.

Lim, C. R., Kimata, Y., Ohdate, H., Kokubo, T., Kikuchi, N., Horigome, T. and Kohno, K. (2000). The Saccharomyces cerevisiae RuvB-like protein, Tih2p, is required for cell cycle progression and RNA polymerase II-directed transcription. *J. Biol. Chem.* **275**, 22409-22417.

Liras, P., McCusker, J., Mascioli, S. and Haber, J. (1978). Characterization of a mutation in yeast causing nonrandom chromosome loss during mitosis. *Genetics* **88**, 651-671.

Mayer, M. L., Pot, I., Chang, M., Xu, H., Aneliunas, V., Kwok, T., Newitt, R., Aebersold, R., Boone, C., Brown, G. W. et al. (2004). Identification of protein complexes required for efficient sister chromatid cohesion. *Mol. Biol. Cell* **15**, 1736-1745.

Murata-Hori, M., Tatsuka, M. and Wang, Y. L. (2002). Probing the dynamics and functions of aurora B kinase in living cells during mitosis and cytokinesis. *Mol. Biol. Cell* **13**, 1099-1108.

Parish, J. L., Bean, A. M., Park, R. B. and Androphy, E. J. (2007). ChlR1 is required for loading papillomavirus E2 onto mitotic chromosomes and viral genome maintenance. *Mol. Cell.* (in press).

Petronczki, M., Chwalla, B., Siomos, M. F., Yokobayashi, S., Helmhart, W., Deutschbauer, A. M., Davis, R. W., Watanabe, Y. and Nasmyth, K. (2004). Sister-chromatid cohesion mediated by the alternative RF-CCtf18/Dcc1/Ctf8, the helicase Chl1 and the polymerase-alpha-associated protein Ctf4 is essential for chromatid disjunction during meiosis II. *J. Cell Sci.* **117**, 3547-3559.

Rajagopalan, H. and Lengauer, C. (2004). Aneuploidy and cancer. *Nature* **432**, 338-341.

Skibbens, R. V. (2004). Chl1p, a DNA helicase-like protein in budding yeast, functions in sister-chromatid cohesion. *Genetics* **166**, 33-42.

Skibbens, R. V. (2005). Unzipped and loaded: the role of DNA helicases and RFC clamp-loading complexes in sister chromatid cohesion. *J. Cell Biol.* **169**, 841-846.

Skibbens, R. V., Corson, L. B., Koshland, D. and Hieter, P. (1999). Ctf7p is essential for sister chromatid cohesion and links mitotic chromosome structure to the DNA replication machinery. *Genes Dev.* **13**, 307-319.

Sonoda, E., Matsusaka, T., Morrison, C., Vagnarelli, P., Hoshi, O., Ushiki, T., Nojima, K., Fukagawa, T., Waizenegger, I. C., Peters, J. M. et al. (2001). Scc1/Rad21/Mcd1 is required for sister chromatid cohesion and kinetochore function in vertebrate cells. *Dev. Cell* **1**, 759-770.

Spencer, F., Gerring, S. L., Connelly, C. and Hieter, P. (1990). Mitotic chromosome transmission fidelity mutants in Saccharomyces cerevisiae. *Genetics* **124**, 237-249.

Stearns, T., Evans, L. and Kirschner, M. (1991). Gamma-tubulin is a highly conserved component of the centrosome. *Cell* **65**, 825-836.

Toth, A., Ciosk, R., Uhlmann, F., Galova, M., Schleiffer, A. and Nasmyth, K. (1999). Yeast cohesin complex requires a conserved protein, Eco1p(Ctf7), to establish cohesion between sister chromatids during DNA replication. *Genes Dev.* **13**, 320-333.

Tuteja, N. and Tuteja, R. (2004). Unraveling DNA helicases. Motif, structure, mechanism and function. *Eur. J. Biochem.* **271**, 1849-1863.

Uhlmann, F. (2004). The mechanism of sister chromatid cohesion. *Exp. Cell Res.* **296**, 80-85.

Uhlmann, F., Lottspeich, F. and Nasmyth, K. (1999). Sister-chromatid separation at anaphase onset is promoted by cleavage of the cohesin subunit Scc1. *Nature* **400**, 37-42.

Uhlmann, F., Wernic, D., Poupart, M. A., Koonin, E. V. and Nasmyth, K. (2000). Cleavage of cohesin by the CD clan protease separin triggers anaphase in yeast. *Cell* **103**, 375-386.

van Brabant, A. J., Stan, R. and Ellis, N. A. (2000). DNA helicases, genomic instability, and human genetic disease. *Annu. Rev. Genomics Hum. Genet.* **1**, 409-459.

Vass, S., Cotterill, S., Valdeolmillos, A. M., Barbero, J. L., Lin, E., Warren, W. D. and Heck, M. M. (2003). Depletion of Drad21/Scc1 in Drosophila cells leads to instability of the cohesin complex and disruption of mitotic progression. *Curr. Biol.* **13**, 208-218.

Waizenegger, I. C., Hauf, S., Meinke, A. and Peters, J. M. (2000). Two distinct pathways remove mammalian cohesin from chromosome arms in prophase and from centromeres in anaphase. *Cell* **103**, 399-410.

Warren, C. D., Eckley, D. M., Lee, M. S., Hanna, J. S., Hughes, A., Peyser, B., Jie, C., Irizarry, R. and Spencer, F. A. (2004). S-phase checkpoint genes safeguard high-fidelity sister chromatid cohesion. *Mol. Biol. Cell* **15**, 1724-1735.

Watanabe, Y. (2005). Sister chromatid cohesion along arms and at centromeres. *Trends Genet.* **21**, 405-412.